



HAL
open science

Structural defects in AFe_2O_4 ($A = Zn, Mg$) spinels

Manuel Gaudon, Nathalie Pailhé, Alain Wattiaux, Alain Demourgues

► **To cite this version:**

Manuel Gaudon, Nathalie Pailhé, Alain Wattiaux, Alain Demourgues. Structural defects in AFe_2O_4 ($A = Zn, Mg$) spinels. *Materials Research Bulletin*, 2009, 44 (3), pp.479-484. 10.1016/j.materresbull.2008.12.005 . hal-00360264

HAL Id: hal-00360264

<https://hal.science/hal-00360264>

Submitted on 24 May 2022

HAL is a multi-disciplinary open access archive for the deposit and dissemination of scientific research documents, whether they are published or not. The documents may come from teaching and research institutions in France or abroad, or from public or private research centers.

L'archive ouverte pluridisciplinaire **HAL**, est destinée au dépôt et à la diffusion de documents scientifiques de niveau recherche, publiés ou non, émanant des établissements d'enseignement et de recherche français ou étrangers, des laboratoires publics ou privés.

Structural defects in AFe_2O_4 ($A = Zn, Mg$) spinels

M. Gaudon*, N. Pailhé, A. Wattiaux, A. Demourgues

Institute of Condensed Matter Chemistry of Bordeaux, ICMCB-CNRS, 87 Avenue Dr. A. Schweitzer, 33608 Pessac cedex, France

ABSTRACT

$(Zn^{2+}/Mg^{2+})[Fe^{3+}]_2O_4$ spinel oxides can be refined as direct/fully inverted (respectively) spinels but considering cationic and anionic vacancies and/or interstitial atoms instead of a partial inversion rate of the A^{2+} and B^{3+} cations. The refinements results of the X-ray diffraction patterns and Mössbauer spectroscopy spectra are discussed and show the veracity of the new structural formalism.

1. Introduction

$A^{2+}(B^{3+})_2O_4$ compounds commonly adopt a cubic symmetry with the $Fd-3m$ space group related to the spinel-type structure. In such a structure, A^{2+} and B^{3+} cations occupy either the octahedral sites (16d) or the tetrahedral sites (8a) depending on their affinity for these various environments. When all the divalent cations are located in the tetrahedral sites, the spinel network is defined as a normal one or a direct one. In some cases, octahedral sites can also be occupied by a fraction or the totality of divalent cations, forcing an equivalent amount of trivalent cations to occupy tetrahedral sites. In such cases, the spinel structure is partially inverted or fully inverted, respectively. Hereafter, the inversion percentage is defined as $100y$, with y the stoichiometric coefficient for the following formulae associated to spinel structure: $A^{2+}_{1-y}B^{3+}_y[A^{2+}_yB^{3+}_{2-y}]O_4$ where square brackets refer to octahedral sites. With the structural convention used in the following, each oxygen atom of the network, common to three octahedral sites (16d sites) and one tetrahedral site (8a sites), is located in 32e sites with spatial coordinates (u, u, u) . In Fig. 1 is presented a typical Fourier cartography for AB_2O_4 spinel composition and for two characteristic plans: $z = 0$ and $z = 1/8$. In spinel framework, the point group symmetry of the tetrahedral sites remains perfectly isotropic, i.e., with Td configuration, whereas the octahedral sites are distorted and exhibit D_{3d} symmetry. Nevertheless, such description results from a global point of view for which the local atomic environments cannot be distinguished while several atoms occupy both tetrahedral and octahedral sites. X-ray data refinements with Rietveld method lead so to limited information: cell parameter, inversion rate and (u, u, u) average position of oxygen anion. All these parameters are known to be

dependant from the composition, the analysis temperature either from the thermal history of the sample: temperature/duration of annealing, thermal cycle rates (quenching) and atmosphere. However some contradictions appear between the observed inversion rate and u parameter. For instance, considering specific literature data devoted to the Mg or Zn ferrite spinels, from numerous refinements, calculated bond distances are not satisfying in regard of the theoretical ones which can be evaluated from the Brown and Altermatt model [1]. Hence, for the $ZnFe_2O_4$ composition which has been described in the literature as partially inverted spinel with a low rate of Fe^{3+} in Td sites, the crystallographic data [2–5] proposed 8a–32e bond distances varying from 1.97 Å to 1.985 Å, i.e., longer than the Zn–O bond distances predicted for 4-coordinated Zn^{2+} sites: 1.962 Å, a partial occupation of this site by the smallest cations (Fe^{3+}) cannot easily be considered.

In the present study, it will be shown that $Zn^{2+}/Mg^{2+}(Fe^{3+})_2O_4$ spinel oxides can be refined considering models including cationic and anionic vacancies and/or interstitial atoms. One can notice that even if, especially for aluminate spinels ($MgAl_2O_4$, $ZnAl_2O_4$), *ab initio* calculations have evidenced the energetic stability of internal cluster formed by recombination of interstitial atoms and atomic vacancies (Frenkel pairs association) [6–8] and so, the possibility of their presence, no experimental refinement were performed including into consideration such phenomena.

Finally, for the $ZnFe_2O_4$ sample, electronic residues in inserted position (48f and 8b sites) have been identified and may explain the distributed cationic vacancies into the (8a) tetrahedral sites.

This work proposes a new view on the cationic distribution into the spinel oxide network allowing to explain the evolution of the bond distances, the inversion rates and the oxygen atom coordinates. The aim of this paper is to compare the standard model: direct/inverted spinel to another formalism taking into account cationic/anionic vacancies with a specific distribution on the various sites.

* Corresponding author. Tel.: +33 5 40 00 66 85; fax: +33 5 40 00 27 61.
E-mail address: gaudon@icmcb-bordeaux.cnrs.fr (M. Gaudon).

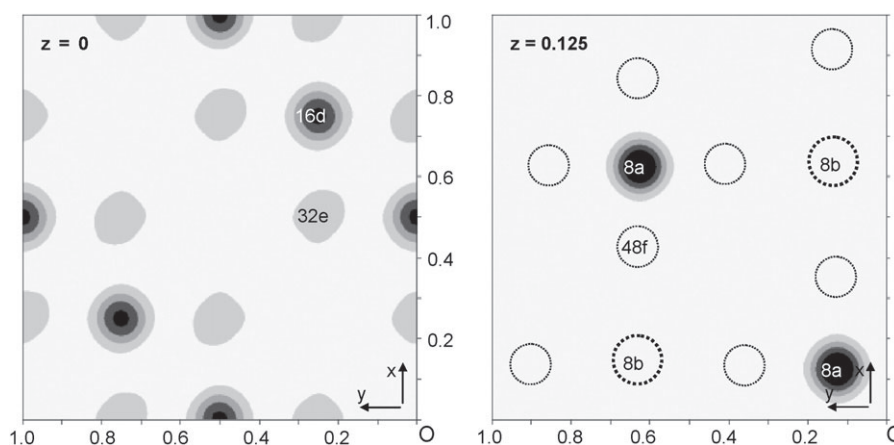


Fig. 1. Spinel electronic cartography of $z = 0$ and $z = 0.125$ plan.

2. Experimental

2.1. Synthesis process

(Zn/Mg)Fe₂O₄ pigments were synthesized by the Pechini route [9]. Aqueous solutions of citrate were prepared by dissolving citric acid (CA) in a minimal volume of water. Then, cationic salts, Fe(NO₃)₃·9H₂O and Mg(NO₃)₂·6H₂O, were added in stoichiometric proportion to the acid solution. A CA:cations molar ratio equal to 3:1 was used. After complete dissolution of metallic salts, ethylene glycol (EG) was added to the mixture under magnetic stirring, with a 4:1 EG:CA molar ratio. EG–CA polymerization was promoted by removing water with continued heating on a hot plate until solutions became highly viscous. Then, the obtained gelled mixtures are thermally treated in ambient atmosphere with two calcination steps: a first “pre-calcination” at 300 °C for 10 h with a heating/cooling rate of 1 °C min⁻¹, then, an annealing for 5 h at 1000 °C with 1 °C min⁻¹ heating/cooling rate was finally performed. This chemical process is used instead of solid state route in order to obtain a higher cationic homogeneity.

2.2. X-ray diffraction studies

For structural investigations, X-ray diffraction (XRD) measurements were carried out on a PANalytical X'PERT PRO diffractometer using Co(Kα₁/Kα₂) radiation in order to suppress any fluorescence problem related to the occurrence of Fe³⁺ ions. The f and f' anomalous dispersion corrections (real and imaginary parts) of each element (O, Fe, Mg, Zn) besides co-radiation, defined from the formulae $f_{at} = f_0 + f' + if''$ where f_{at} is the atomic scattering factor [10], were manually introduced into the program. XRD data were recorded with a 2θ step = 0.017° with a counting time over 200 s per step and 10–120° 2θ range. The patterns have been treated using Rietveld refinement method using FULLPROF[®] program suite [11–12]. The diffraction peaks profiles were approximated as a pseudo-Voigt using Caglioti function. The refined parameters are zero shift, scale factor, background polynomial parameters, peaks profile parameters U , V , W , and η (Lorentzian/Gaussian distribution), unit cell parameters, atomic positions, site occupancies and isotropic displacement factors.

2.3. Mössbauer studies

In order to evaluate Fe³⁺ local environments and magnetic ordering of the studied ferrite compounds, ⁵⁷Fe Mössbauer measurements were performed at 293 K and 4 K. Both analyses are in transmission mode and were made using a conventional

constant acceleration spectrometer (HALDER) using rhodium matrix source. The fitting of Mössbauer patterns as a series of Lorentzian profile peaks allowed the calculation of position (δ), amplitude and width (I) of each peak: thus, experimental hyperfine parameters were determined for the various iron sites by least square program.

3. Results and discussion

3.1. Focus on MgFe₂O₄ composition

For X-ray refinements performed on MgFe₂O₄ compound, whatever the refinement process used, cell parameter, peak profile decentring and background coefficient do not vary significantly and are not here discussed. Unit cell parameter remains equal to 8.3930(1) Å, a value in good agreement (but corresponding to the higher values) with the literature data [13–15].

As “reference”, the structural hypothesis for refinement corresponds to fully inverted spinel without any cationic/anionic vacancy. The refinement results are reported in Table 2. This model is deficient since the isotropic displacement factors are not satisfying with negative values refined for 16d site cations. Obviously, the isotropic displacement factors of the 16d sites exhibit negative values because of their electronic density is too low with this structural hypothesis. The standard way to optimize this electronic filling in the spinel network is to consider partially inverted spinel (Mg atoms: $z = 12$ contain twice less electrons than Fe ones: $z = 26$). Results obtained from this free cationic distribution, joined in Table 2, clearly show a very important improvement of the refinement in comparison with the fully inverted model. The various correlation factors: Rp, Rwp, Rexp, RBragg indicate a “satisfying” refinement. The RBragg factor, characteristic of the structural refinement quality, has notably decreased from 7.5% to 3.4%. The partial inversion rate (79%) and the (u , u , u) anion's position are consistent with those proposed in current literature [13,16–18]. Hence, one may conclude that the MgFe₂O₄ is a partially inverted spinel, nevertheless, several points are unclear.

Firstly, the isotropic displacement factors (B_{iso}) of the cations in the tetrahedral sites are slightly larger to those in the octahedral sites. Actually, one can consider that octahedral sites should exhibit a larger B_{iso} values than tetrahedral sites ones because of its longer bond lengths and also because the octahedral sites are occupied by a large content of Mg²⁺ ions which are the lighter cations.

Secondly, the metal–ligand bond lengths have been checked and compared with the theoretical ones which can be predicted

Table 1

M–O bonds lengths (and standard deviation) estimated from the Brown and Altermatt law.

M–O bonds	Theoretical lengths	Experimental average lengths in MgFe ₂ O ₄ /in ZnFe ₂ O ₄
Site 8a	Mg–O: 1.949 Å; Zn–O: 1.962 Å; Fe–O: 1.865 Å	A–O: 1.948 Å/1.974 Å
Site 16d	Mg–O: 2.099 Å; Zn–O: 2.110 Å; Fe–O: 2.015 Å	B–O: 2.026 Å/2.030 Å

basing on the Brown and Altermatt semi-empirical law [1]. This equation is normally used in order to check if the distances established by diffractograms refinement are correct. Here, this law was used in a reverse way in order to deduce from the valences of each element, the theoretical metal–cation bond lengths in various environments. Theoretical M–O lengths are reported in Table 1. From these M–O lengths it is possible to now predict the theoretical inversion rate that one should have obtained in order to satisfy the experimental M–O distances (deduced from the refinement). Here, considering a mixing law between Mg–O and Fe–O theoretical bond lengths and with an inversion percentage of 79%, 1.883 Å and 2.048 Å lengths should be obtained, respectively for tetrahedral and octahedral sites. The calculated distances from refinements are 1.948 Å and 2.026 Å for tetrahedral and octahedral sites, respectively, i.e., too high and too low considering the bond distances estimated on the basis of the Brown model. However, it can be noticed these distances are “standard” in regard of the literature data.

Thus, the following hypothesis has been considered: the atomic distribution in the MgFe₂O₄ spinel may quite remain fully inverted but in addition cationic/anionic vacancies have to be taken into account in order to explain the experimental bond distances. This hypothesis also means that the inversion rate proposed in the literature is actually an artefact issued from the inconsideration of vacancies mainly located on the tetrahedral sites of the structure.

Fe_{1–3x}[Mg_{1–x}Fe_{1+x}]O_{4–4x} formulae was envisaged on the basis of the chemical composition, a complete filling of the octahedral sites and the oxide electroneutrality. Note that a partial occupation of the octahedral sites by Mg²⁺ has to be considered. There is the same number of adjustment parameters in this case than for the inversion rate model: *x* variable directly replacing the *y* inversion rate variable, i.e., the reliability factors issued from both model can be directly compared. The refinement was illustrated in Fig. 2a exhibiting experimental, calculated and difference signals. The results of the refinements are reported in Table 2; the experimental bond lengths found with this last refinement model were joined to Table 1. The *x* vacancy was determined and found equal to 0.04. This last model leads to the weakest correlation factors, particularly for the R_{Bragg} factor. Furthermore, the cationic isotropic displacement factors are now more consistent. Indeed, the *B*_{iso} coefficients of the octahedral sites became slightly higher than the tetrahedral sites ones. However one should notice that *B*_{iso} value of the oxygen atom remains low. Moreover, even if the two last refinement models (with or without vacancies) are very different, the electronic residues are distributed in the two cases in a very similar way. This phenomenon is illustrated by the Fourier maps (Fobs–Fcal) reported in Fig. 3. In addition the Fourier map established from the purely inverted and non-lacunar spinel model has been reported in order to illustrate the large improvement of the refinement quality from this first model up to the last one. For the as-prepared MgFe₂O₄ oxide, the consideration of vacancies segregated on tetrahedral positions leads to the same results than those obtained with the partial inversion of Fe³⁺ ions in tetrahedral sites.

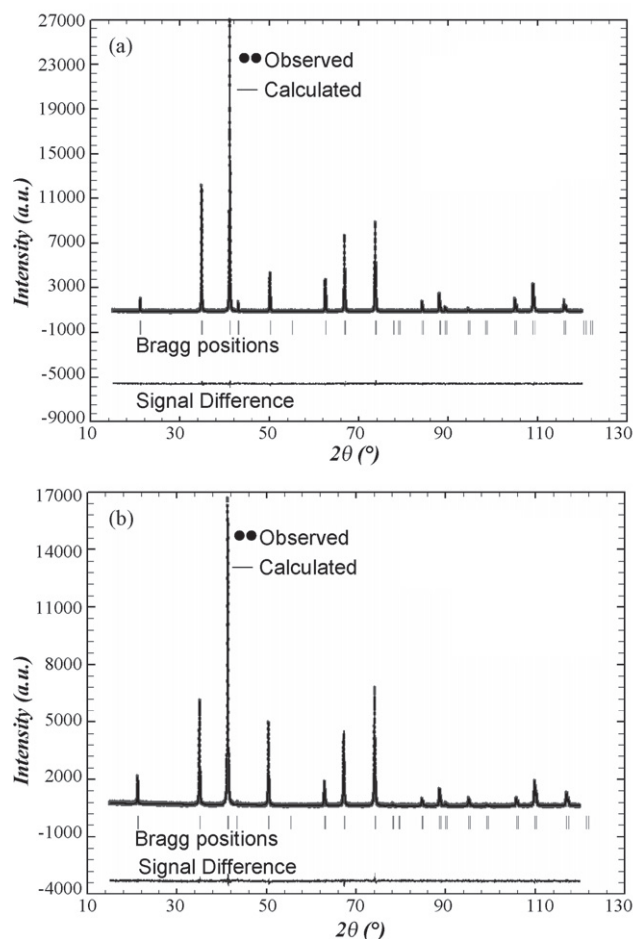


Fig. 2. Experimental, calculated and difference signals for MgFe₂O₄ (a) and ZnFe₂O₄ (b) oxides refined with the lacunar models.

3.2. Focus on ZnFe₂O₄ composition

A comparable study to the previous one was performed on ZnFe₂O₄ composition. In the literature data [2–5], this composition is referred as quasi-direct spinel, i.e., with a weak inversion rate ranging from 5% to 15% depending on the authors. Studies have

Table 2

Refined structural parameters for MgFe₂O₄ considering the various cationic distribution models.

Atom	Site	<i>x</i>	<i>y</i>	<i>z</i>	<i>B</i> _{iso} (Å ²)	SOF
MgFe ₂ O ₄ refined as fully inverted spinel ^a						
Fe1	8a	1/8	1/8	1/8	1.6(2)	1
Mg2	16d	1/2	1/2	1/2	–0.3(1)	0.5
Fe2	16d	1/2	1/2	1/2	–0.3(1)	0.5
O	32e	0.2590(4)	<i>x</i>	<i>x</i>	0.1(2)	1
MgFe ₂ O ₄ refined as partially inverted spinel ^b						
Mg1	8a	1/8	1/8	1/8	0.54(7)	0.210(6)
Fe1	8a	1/8	1/8	1/8	0.54(5)	0.790(6)
Mg2	16d	1/2	1/2	1/2	0.43(6)	0.395(3)
Fe2	16d	1/2	1/2	1/2	0.43(6)	0.605(3)
O	32e	0.2560(2)	<i>x</i>	<i>x</i>	0.49(8)	1
MgFe ₂ O ₄ refined as Fe _{1–3x} [Mg _{1–x} Fe _{1+x}]O _{4–4x} ^c						
Fe1	8a	1/8	1/8	1/8	0.44(5)	0.87(1)
Mg2	16d	1/2	1/2	1/2	0.52(4)	0.48(1)
Fe2	16d	1/2	1/2	1/2	0.52(4)	0.52(1)
O	32e	0.2560(2)	<i>x</i>	<i>x</i>	0.29(7)	0.96(1)

^a Rp = 3.56%; Rexp = 3.49%; Rwp = 4.73%; RBragg = 7.5%.

^b Rp = 2.76%; Rexp = 3.64%; Rwp = 3.50%; RBragg = 3.55%.

^c Rp = 2.64%; Rexp = 3.49%; Rwp = 3.37%; RBragg = 2.86%.

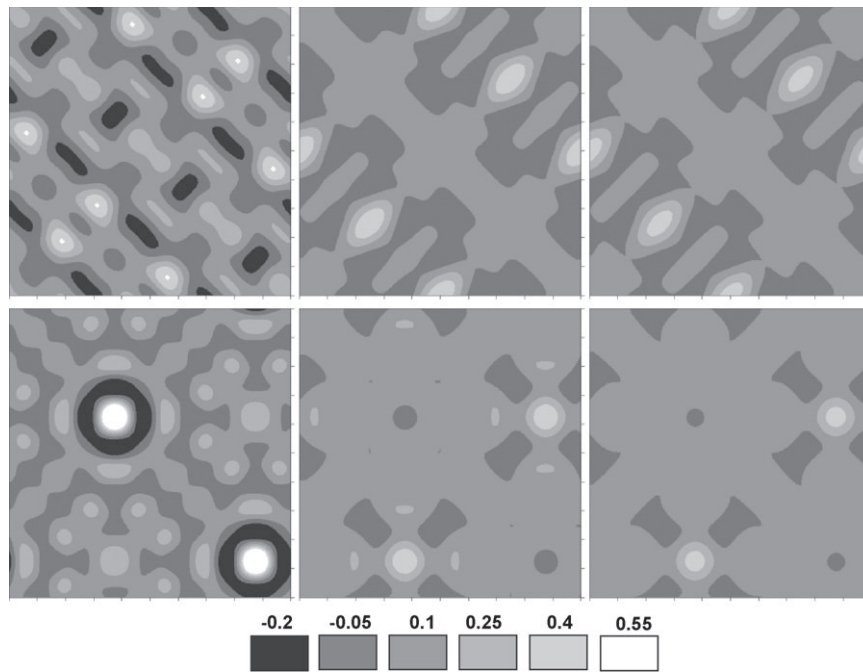


Fig. 3. Fourier cartographies (Fobs–Fcal) of $z = 0$ (top) and $z = 0.125$ (bottom) planes of the MgFe_2O_4 oxide. They are respectively from left to right obtained considering a fully inverted, a partially inverted or a partially lacunar model.

notably show that the inversion rate depends on thermal sample history [19]. On the contrary, Mössbauer studies show that even if nano-sized particles obtained with ball-milling or by sweet chemistry routes (sol–gel) exhibit high degree of inversion, particles with grain size over 10 nm exhibit no magnetic super-exchange and can so be considered as purely normal spinel [20–22]. This so consist in an unclear point in the literature.

Firstly, refinements have been performed considering spinel as a direct one. Secondly, the inversion rate between A and B sites cations was refined. Whatever the refinement model, the cell parameter is found equal to 8.4424 Å. Same observations can be made than for MgFe_2O_4 study. There is a very significant improvement between the direct and partially inverted spinel model (Table 3 refinement results); nevertheless several points have to be discussed such as displacement factors as well as M–O bond lengths. Actually, the $M_{\text{Td}}\text{–O}$ distances are more important than those established from Brown and Altermatt for a pure direct spinel, i.e., $\text{Zn}_{(\text{IV})}\text{–O}$ bonds lengths (1.978 Å instead of 1.962 Å). Consequently, it is less probable that a part of the Td site is occupied by a fraction of Fe^{3+} ions, these last cations being largely smaller than Zn^{2+} ones.

As for MgFe_2O_4 , a model where vacancies are mainly segregated on the tetrahedral sites has to be rather considered. In comparison with the MgFe_2O_4 compound, for ZnFe_2O_4 composition, a vacancy rate on tetrahedral site implies in order to maintain the Fe/Zn molar ratio that a part of zinc migrates on 16d sites. Then, the refinement was performed considering the $\text{Zn}_{1-3x}[\text{Fe}_{2-2x}\text{Zn}_{2x}]\text{O}_{4-4x}$ formula. The refinement patterns are reported in Fig. 2b. This oxide formula was established with a part of Zn^{2+} ions located in 16d sites without any compensation by the migration of Fe^{3+} through 8a sites but, on the contrary, considering only compensation by oxygen vacancy creation. The corresponding refinement results are reported in Table 3 and are comparable with the partially inverted spinel model. Moreover, whatever the refinement model which is chosen, the Fourier maps show non-negligible electronic residues on two inserted positions: the 48f sites and especially on 8b sites (see Fig. 4). Thus, it seems that the occurrence of Zn^{2+} ions in the octahedral sites may be the cause (consequence?) of a local structural reorganiza-

tion. In a first time, it is interesting to know which elements (cations or oxygen anions) can be located into the interstitial sites. All the possible hypotheses were envisaged and discussed examining the consequence of the filling of these interstitial sites by various elements on the bonds and sites valences. The hypothesis of a settlement of 8b or 48f sites by cations (as well Fe^{3+} as Zn^{2+}) could be eliminated since the occurrence of 8b cations would lead to the disappearance of the four first-neighbouring 16d sites because of the creation of too short M–M chemical bonds (face-sharing octahedral

Table 3

Refined structural parameters for ZnFe_2O_4 considering the various cationic distribution models.

Atom	Site	x	y	z	B_{iso} (Å ²)	SOF
ZnFe₂O₄ refined as direct spinel^a						
Zn1	8a	1/8	1/8	1/8	1.09(6)	1
Fe2	16d	1/2	1/2	1/2	–0.36(6)	1
O	32e	0.2612(4)	x	x	0.2(2)	1
ZnFe₂O₄ refined as partially inverted spinel^b						
Zn1	8a	1/8	1/8	1/8	0.41(4)	0.140(6)
Fe1	8a	1/8	1/8	1/8	0.41(4)	0.860(6)
Zn2	16d	1/2	1/2	1/2	0.47(5)	0.930(3)
Fe2	16d	1/2	1/2	1/2	0.47(5)	0.070(3)
O	32e	0.2603(2)	x	x	0.82(6)	1
ZnFe₂O₄ refined as $\text{Zn}_{1-3x}[\text{Zn}_{2x}\text{Fe}_{2-2x}]\text{O}_{4-4x}$^c						
Zn1	8a	1/8	1/8	1/8	0.48(3)	0.946(7)
Zn2	16d	1/2	1/2	1/2	0.40(4)	0.018(4)
Fe2	16d	1/2	1/2	1/2	0.40(4)	0.982(4)
O	32e	0.2603(2)	x	x	0.81(6)	0.98(1)
ZnFe₂O₄ refined as “defect” $\text{Zn}_{1-3x}[\text{Zn}_{2x}\text{Fe}_{2-2x}]\text{O}_{4-4x}$^d						
Zn1	8a	1/8	1/8	1/8	0.42(3)	0.936(7)
Zn2	16d	1/2	1/2	1/2	0.48(4)	0.021(4)
Fe2	16d	1/2	1/2	1/2	0.48(4)	0.979(4)
Oi1	8b	0.625	1/8	1/8	0.78(6)	0.010(2)
Oi2	48f	0.3436	1/8	1/8	0.78(6)	0.003(1)
O	32e	0.2599(2)	x	x	0.78(6)	0.97(1)

^a Rp = 2.64%; Rexp = 3.03%; Rwp = 3.39%; RBragg = 5.07%.

^b Rp = 2.30%; Rexp = 3.13%; Rwp = 2.92%; RBragg = 2.26%.

^c Rp = 2.30%; Rexp = 3.13%; Rwp = 2.86%; RBragg = 2.28%.

^d Rp = 2.23%; Rexp = 3.03%; Rwp = 2.84%; RBragg = 2.03%.

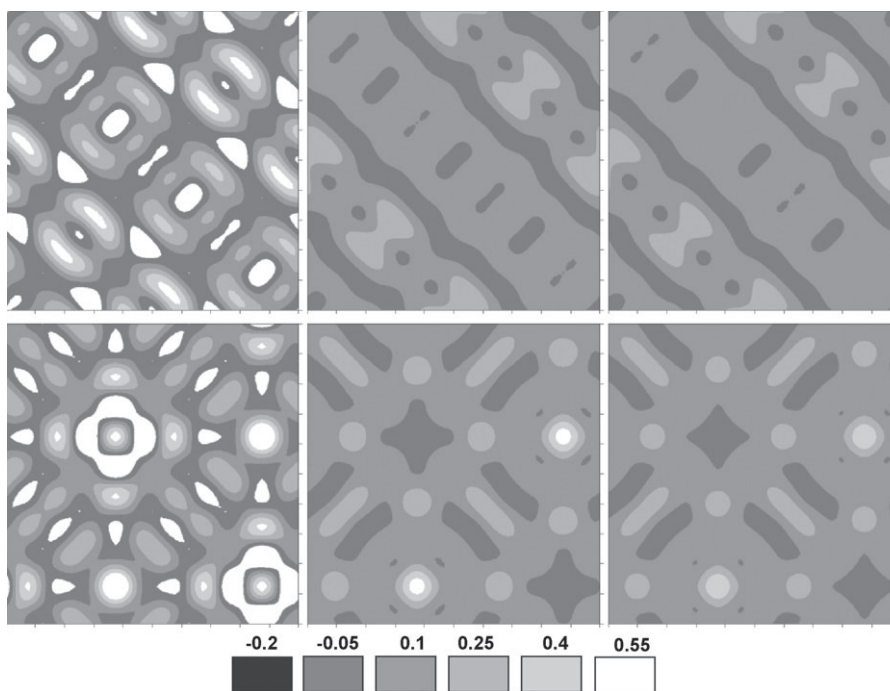


Fig. 4. Fourier cartographies (Fobs–Fcal) of $z = 0$ (top) and $z = 0.125$ (bottom) plans of the ZnFe_2O_4 oxide. They are respectively from left to right obtained considering a direct, a partially inverted or a partially lacunar model.

and tetrahedral cationic sites never existing). Such reorganization would so imply too expensive crystallographic network reorganization from an energetic point of view. Then, other solutions can be envisaged for the 8b/48f settlements: (i) to consider a reorganization around an isolated defect, (ii) to build small clusters constituted from recombination of several 8b/48f inserted anions (the consideration of clusters as possible defect goes in the direction of the studies drawn up from *ab initio* calculations [8]), or (iii) to consider that the 8b/48f anions can be located at the surface of the oxides.

For instance, we tried to illustrate possible network reorganization around an inserted 8b anion. The occurrence of extra 8b anions implies for the anion valence bond satisfaction and in order to limit network reorganization, the cationic filling of the four first 16d neighbours by Zn^{2+} ions substituting for Fe^{3+} ones. Moreover, the settlement of 8b site with an oxygen anion implies the disappearance of the four 32e first neighbours involving the disappearance of half of the six corners of the four 16d neighbours. Thus, the 16d neighbours become 4-coordinated (distorted tetrahedral sites) with three of their corners are 32e oxygen and one is the 8b inserted anion. A valence calculation of these “modified” 16d sites shows it can correspond to stabilization of Zn^{2+} cations. Furthermore, this fourfold coordination is really consistent with the strong preference of the Zn^{2+} cation for tetrahedral symmetry. The anion sub-network modification is compatible with the replacement of four 16d Fe^{3+} cations by Zn^{2+} cations which occupied preferentially the 8a sites. The 8a sites filled by Zn^{2+} cations are probably the four ones affected by the elimination of the four 32e anions which are 8b sites first neighbours. Furthermore, the proposed cluster explains the source of the defect formation, i.e., the positioning and the energetic stability of the Zn^{2+} cations on 16d “tetrahedral” sites.

The validation of this structural hypothesis (anions insertion on 8b/48f sites) comes from the significant improvement of the refinement with a model with one 8b sites for two 48f sites. The chosen code for each site occupancies corresponds to the composition feature $\text{Zn}_{1-3x}[\text{Zn}_{2x}\text{Fe}_{2-2x}]\text{O}^{(32e)}_{4-5.5x}\text{O}^{(8b)}_{0.5x}\text{O}^{(48f)}_x$;

this code was established after a preliminary refinement performed on all occupancies. Moreover, this refinement procedure does not introduce supplementary adjustment parameters and can be directly compared with the previous ones. Notably, the RBragg factor decreases from 2.28% from the previous model until 2.03% for this last one. Furthermore, the isotropic displacement factors of the 16d and 8a positions become now correct considering the M–O bond distances and the electronic occupancies of the 8a and 16d sites (8a are the smallest sites occupied by the louder atoms).

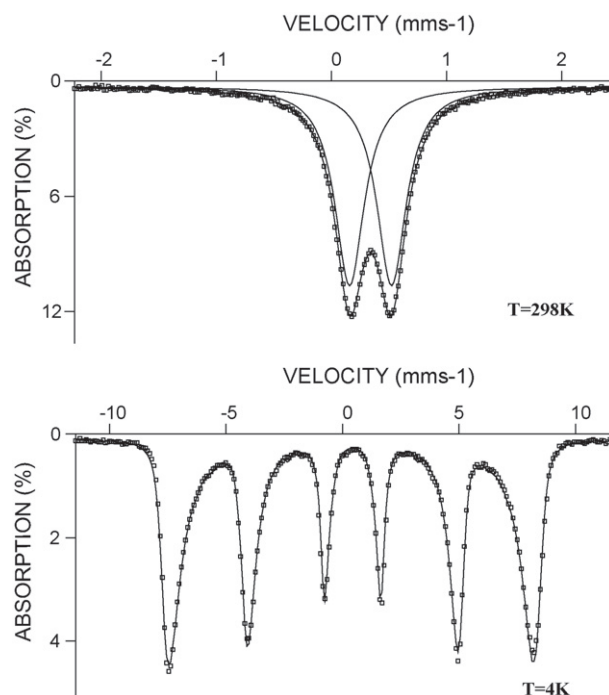


Fig. 5. Mössbauer spectra of the ZnFe_2O_4 powder.

Table 4Refined Mössbauer parameters on the ZnFe₂O₄ powder.

Temperature	Site	δ (mm/s)	Δ (mm/s)	Γ (mm/s)	ε (mm/s)	H^* (T)
4 K	1	0.349	0.366	0.310	–	–
298 K	1	0.45	–	0.35	–0.029	47.8

On the ZnFe₂O₄ spinel composition, Mössbauer analyses were also performed at 4 K and 298 K (spectra being reported in Fig. 5). At 4 K, the signal shows a sextuplet characteristic of anti-ferromagnetic order, and at 298 K, the signal shows a quadripolar doublet characteristic of a paramagnetic behaviour. The parameters of fitting are reported in Table 4. For both temperature, only one site is visible, the signal exhibiting only one contribution; the parameters relative to this site (hyperfine mean field value refined at 4 K is about 48 T) being characteristic of sixfold coordination. For the sample analysed at 4 K, even if the Mössbauer signal is fitted with a double contribution, these two contributions converge through quite same hyperfine parameters relative to octahedral sites hence showing the absence of any tetrahedral sites contribution. Thus, Mössbauer analyses tend to confirm the structural hypothesis of a lacunar but direct contribution for the ZnAl₂O₄ spinel feature.

4. Conclusion

Herein it was proposed a new view of the ferrites networks (MgFe₂O₄/ZnFe₂O₄) taking into account the occurrence of cationic vacancies in Td sites. In order to respect the chemical composition, the presence of these vacancies forces the framework to accept divalent cations in 16d sites which are formally octahedral environments and the occurrence of oxygen vacancies and/or oxygen in interstitial sites in order to limit energetic destabilization in clusters. These oxygen defects lead to consider that some

ions in 16d site, probably Zn²⁺ in the case of ZnFe₂O₄ or even Fe³⁺ ions in the case of MgFe₂O₄ compound, are not in octahedral site but fourfold coordinated to oxygen in a strongly distorted tetrahedral site. After refinement by the Rietveld method and Mössbauer characterisation, our proposed model seems more realistic than the classical fully or partially inverted spinel models previously described in the literature.

References

- [1] I.D. Brown, D. Altermatt, *Acta Crystallogr. B* 41 (1985) 244.
- [2] B. Antic, A. Kremenovic, A.S. Nikolic, M. Stoiljkovic, *J. Phys. Chem. B* 108 (2004) 12646.
- [3] E. Moran, C. Blesa, M.E. Medina, J.D. Tornero, N. Menendez, U. Amador, *Inorg. Chem.* 41 (2001) 5961.
- [4] J.C. Waerenborgh, M.O. Figueiredo, J.M.P. Cabral, L.C.J. Pereira, *J. Solid State Chem.* 111 (1994) 300–309.
- [5] W. Schiessl, W. Potzel, H. Karzel, M. Steiner, G.M. Kalvius, A. Martin, M.K. Krause, R. Wäppling, *Phys. Rev. B* 53 (1996) 9143.
- [6] H. Moriwake, I. Tanaka, F. Oba, Y. Koyama, H. Adachi, *Phys. Rev. B* 15 (2002) 1531031–1531034.
- [7] S.S. De Souza, A.R. Blak, *Radiat. Eff. Defects Solids* 146 (1998) 123.
- [8] J.A. Ball, S.T. Murphy, R.W. Grimes, D. Bacorisen, R. Smith, B.P. Uberuaga, K.E. Sickafus, *Solid State Sci.* 10 (2008) 717–724.
- [9] N. Pechini, Patent No. 3,330,697 (1967).
- [10] A.J.C. Wilson, E. Prince (Eds.), *International Tables of Crystallography*, vol. C, Kluwer Academic Publishers, London, 1999.
- [11] H.M. Rietveld, *Acta Crystallogr.* 22 (1967) 151.
- [12] H.M. Rietveld, *J. Appl. Crystallogr.* 2 (1969) 65.
- [13] H.S.C. O'Neill, H. Annersten, D. Virgo, *Am. Mineral.* 77 (1992) 725.
- [14] J. Podworny, *Appl. Crystallogr.* 17 (1998) 97.
- [15] B.I. Pokrowskii, A.K. Gapeev, K.V. Pokholov, L.N. Komissarova, I.V. Igonina, A.M. Babeshkin, *Kristallografiya* 17 (1972) 793.
- [16] A. Pradeep, P. Priyadharsini, G. Chandrasekaran, *J. Magn. Magn. Mater.* 320 (21) (2008) 2774–2779.
- [17] V.K. Mittal, S. Bera, R. Nithya, M.P. Srinivasan, S. Velmurugan, S.V. Narasimhan, *J. Nucl. Mater.* 335 (2004) 302.
- [18] R.J. Harrison, A. Putnis, *Phys. Chem. Miner.* 26 (1999) 322.
- [19] H.S.C. O'Neill, *Eur. J. Mineral.* 4 (1992) 571.
- [20] F.S. Li, L. Wang, J.B. Wang, Q.G. Zhou, X.Z. Zhou, H.P. Kunke, G. Williams, *J. Magn. Magn. Mater.* 268 (2004) 332–339.
- [21] G.F. Goya, H.R. Rechenberg, *J. Magn. Magn. Mater.* 196–197 (1999) 191.
- [22] L. Wang, Q. Zhou, F. Li, *Phys. Stat. Sol. B* 241 (2004) 377.